Macromolecules

Coil−Globule Transition of a Water-Soluble Polymer

Jianyu Liu, Huazhang Guo, Qingjie Gao, Hongbin Li, Zesheng An, and Wenke Zhang*

Cite This: *Macromolecules* 2022, 55, 8524−8532

Read Online

ACCESS | 📊 Metrics & More | 📑 Article Recommendations | 🆘 Supporting Information

ABSTRACT: The coil−globule transition is a fundamental issue in polymer science and key to the performance of many smart materials. However, an experimental study on the globule structure and real-time dynamics of transition remains a challenge. Using single-molecule magnetic tweezers (MT) and atomic force microscopy (AFM) imaging, the temperature- and solvent-dependent transition of poly(N-isopropylacrylamide) (PNIPAM) single chain, a water-soluble thermoresponsive polymer, is directly observed under an external force. Surprisingly, the globule structure is composed of quantized beads with a basic/ minimum size of ~31 repeat units. Our results indicate that upon heating or salt concentration change, the PNIPAM coil first forms a series of nuclei each consisting of ~31 repeat units, rather than random sizes. The subsequent transition involves a mergence of adjacent beads. Finally, the beads gradually stack to form a loose spheroidal aggregate, rather than a uniform compact globule. The distinct collapsing rates and mechanical stabilities for different collapsed structures are identified for the first time.
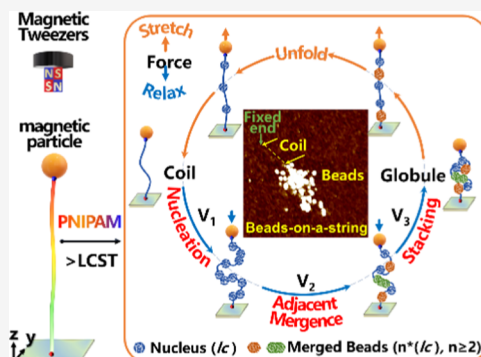
INTRODUCTION

The coil−globule conformational transition of a polymer chain is a fundamental issue in polymer science. It is also one of the key factors that determine the performance of many smart materials and thus has attracted widespread interest across multidisciplinary fields.[1−7] A single-molecule experimental study on the coil−globule transition of purely hydrophobic polymers, such as polystyrene, has been performed success-fully.[8,9] However, such attempts on the study of water-soluble polymers have been unsuccessful to date. Poly(N-isopropyla-crylamide) (PNIPAM) is one of the most widely studied thermoresponsive polymers.[10] PNIPAM has both hydrophilic (amide group) and hydrophobic moieties (isopropyl group) that can form a hydration shell and an intramolecular hydrogen bond and exhibits lower critical solution temperature (LCST) in aqueous solution. At low temperatures and in good solvents, PNIPAM has an extended coil conformation, while at high temperatures and in poor solvents PNIPAM exists as a collapsed globule. The current theory of coil−globule transition for PNIPAM consists of a random-size nucleation process, in which the structures were not identified, and a coarsening process, in which nuclei larger than the critical size continued to swallow in its connected adjacent unwound segments to ultimately form a single uniform globule, whereas nuclei smaller than the critical size dissolved into unwound segments.[11−13] However, some recent research shows the radius of gyration that is the main basis of the present theory is an unsuitable coordinate to comprehend the transition kinetics because it does not capture the high conformational diversity within different states.[14] How a single polymer chain transforms dynamically remains unknown because there is no experimental evidence for the actual structures that form during nucleation and coarsening or in the final globule. Single-molecule force spectroscopy (SMFS), which is based on atomic force microscopy (AFM), optical or magnetic tweezers, is a powerful tool for the study of individual polymer chains.[15−21] However, due to issues associated with instrument sensitivity and sample preparation, the AFM-based SMFS studies of PNIPAM have produced contradictory results, and some researchers claimed the observation of a compact globule, while others believed that the coil−globule transition of PNIPAM was undetectable by AFM-SMFS.[22−26]

To visualize the coil−globule transition in real time, we monitored the end-to-end distance change of a PNIPAM chain using magnetic tweezers (Figure 1A) (for more details, see Materials and Methods section) that possesses higher force sensitivity and long-term stability in comparison with AFM-SMFS.[27−35] For the temperature-driven experiment (T), the chain was allowed to collapse freely (i.e., no external force) at 42.5 °C and then stretched by a constant force of 6 pN at 42.5 °C (R0-T6) (Figure 1B). Interestingly, the extension curves of collapsed globules were discontinuous and showed multiple wait-and-jump steps with different jump lengths (Figure 1C,D).
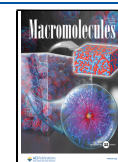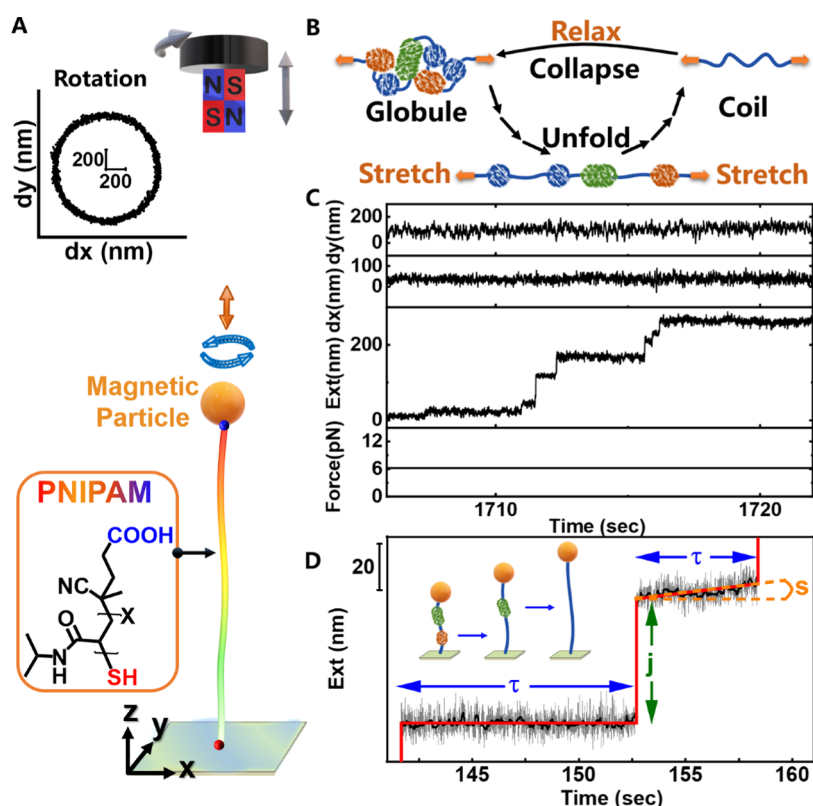
**Figure 1.** Unfolding of collapsed individual PNIPAM chains using single-molecule magnetic tweezers (MT) in constant force mode. (A) Scheme of the MT measurement of a single polymer chain tethered between the coverslip and the magnetic particle. The perfect circular trajectory of the tethered magnetic particle (see the inset) observed when rotating the magnets proves the single-molecule manipulation. (B) Diagram of the stretching−relaxation response of a PNIPAM chain under coil−globule transition conditions. The blue, orange, and green blobs represent beads of different sizes. (C) Typical traces obtained during the unfolding of collapsed PNIPAM under a constant force of 6 pN at 42.5 °C (R0-T6). From the bottom up, the traces correspond to force-, extension-, d x- and d y-vs-time trajectories. The extension, d x, and d y indicate the z, x, and y center positions of the tethered magnetic particle. Multiple jump steps can be observed in the extension−time trace. (D) Magnification of the extension−time trace with the smoothed (black) and reconstituted trajectories (red). The jump length j, waiting time τ, and slope s are defined here.
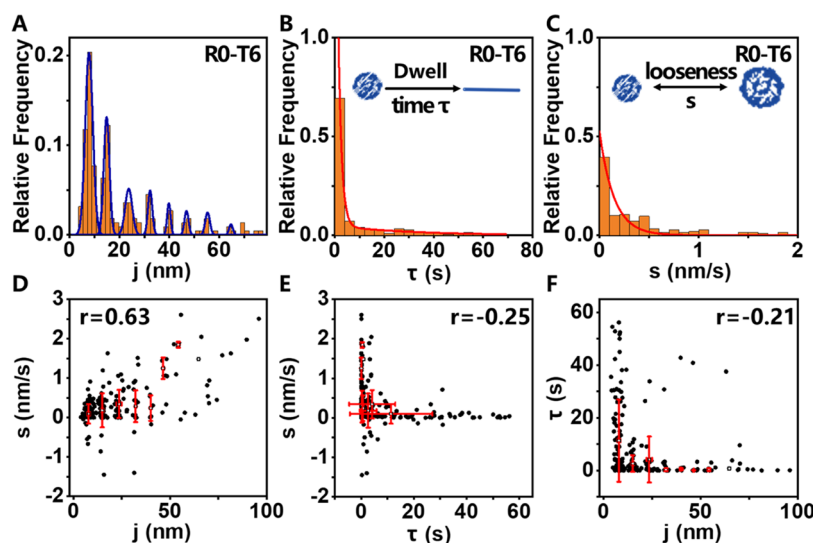
Figure 2. Statistical analysis of the unfolding parameters of the temperature-driven (T) collapse of PNIPAM under a constant force of 6 pN, 42.5 °C (R0-T6). (A) Histograms of the jump length j from 221 jump events. The blue lines show Gaussian fits. (B) Histograms of the unfolding waiting time τ of collapsed structures. The red line shows a double exponential fit. (C) Histograms of the expansive slope s under 6 pN. The red line shows a single exponential fit. (D−F) Correlation plots and Pearson's correlation coefficients (r) of (D) $j − s$, (E) $\tau − s$, and (F) $j − \tau$ from the collapsed polymer under 6 pN. Each black dot represents one wait-and-jump event. The open red squares indicate averages from each peak position in panel (A). The horizontal and vertical error bars indicate standard deviations.

In contrast, the extension remained constant at room temperature (below the LCST) (Figure S1). These multiple steps indicate the real-time force-induced unfolding of collapsed globules, which is similar to the sequential unfolding of the polyprotein beads within the beads-on-a-string structure.[36,37] As shown in Figure 1C, the wait-and-jump steps exhibit different jump lengths (j), waiting times (τ), and slopes (s) (Figure 1D and Supporting Information Section 1.11). We analyzed these parameters systematically to describe the collapsed structures and coil−globule transition.

■ RESULTS AND DISCUSSION

Force-Induced Unfolding of a Collapsed Globule Formed by the Temperature-Driven (R0-T6) Coil−Globule Transition. As shown in Figure 2A, distinct peaks (maxima) at equal jump lengths were observed. The peak positions correspond to the most probable jump length of the collapsed structures. Considering the fact that the end-to-end distance in a poor solvent is much smaller than the theoretical value of $H \sim 1.4$ nm (SI Section 1.12), the jump length here is considered to be the actual size of the collapsed structure. For the temperature-driven transition (R0-T6), the jump length at the first peak was found to be 7.8 ± 1.5 nm, which is equivalent to 31 ± 6 repeat units. The remaining peaks (j) are approximately multiples of the first peak (Figure 2A, SI Section 1.13, and Table 1).

Table 1. Jump Length and the Corresponding Number of Repeated Units of the Temperature-Driven Collapsed PNIPAM Structure Measured at 42.5 °C under an External Force of 6 pN (R0-T6)[a]

peak number (R0-T6)	jump length (nm)	number of repeated units	expected number of repeated units (multiple × nucleus)
1	7.8 ± 1.5	31 ± 6	31 (1 × nucleus)
2	14.9 ± 1.1	59 ± 4	62 (2 × nucleus)
3	23.7 ± 2.4	94 ± 10	93 (3 × nucleus)
4	32.3 ± 0.5	128 ± 2	124 (4 × nucleus)
5	39.8 ± 0.6	158 ± 2	155 (5 × nucleus)
6	46.9 ± 0.6	186 ± 2	186 (6 × nucleus)
7	55.3 ± 0.2	219 ± 1	217 (7 × nucleus)
8	64.7 ± 0.6	257 ± 2	248 (8 × nucleus)

[a]The jump length j is measured and analyzed statistically from extension−time curves of single-molecule magnetic tweezers. The number of repeated units is determined according to the jump length. The smallest jump length is regarded as the size of the nucleus, and the other bigger jump lengths were found to be comparable with the length of multiple nuclei (i.e., the expected number of repeated units).

It should be emphasized that it is normally difficult to unfold tandem repeat structures simultaneously due to tiny local differences.[36,37] Herein, the structure corresponding to the first peak is designated as the nucleus. This is the first time that the basic structure of stable, collapsed PNIPAM has ever been determined experimentally, and the structure agrees well with recent theoretical simulations. These simulations have shown that PNIPAM chains of less than 30 or 32 repeating units are too short to fold.[38−41] Due to the presence of the hydrophobic moiety (e.g., the isopropyl group) and the hydrogen bond donor and acceptor, it is very likely that the PNIPAM chain forms a folding structure via intramolecular hydrogen bonds above LCST. Collapsed structures with multiple nucleus lengths are called merged beads; adjacent nuclei merge to form merged beads and the free segments between the adjacent nuclei are small. This process, named adjacent mergence, differs substantially from the current understanding of nucleus growth, where repeat units in the coil are one by one assimilated into a nucleus of random size. There are two possible reasons that can cause adjacent mergence: (1) the confined space between the adjacent structures can facilitate the contact of structures, therefore, increasing the chance of mergence during collapse[42] and (2) there may exist some defects (e.g., incomplete water layers) at the bead-linear chain interface, which facilitate adjacent bead mergence.

The waiting time τ between successive unfolding steps is the lifetime and reflects the structure's kinetic stability under 6 pN. Our results show that τ follows a multiexponential distribution (at least two exponents) (Figure 2B), suggesting that the unfolding kinetics involves multiple rate-limiting steps. The average waiting time was $\sim$7.4 s, corresponding to an unfolding rate of $\sim$0.14 s^{-1}. Moreover, because the slope s corresponds to a bead's expansion rate in the physical dimension during the force-induced globule-to-coil transition, it reflects structural looseness. The positive s represents expansion. The expansive slope exhibits an exponential distribution (Figure 2C). For the individual wait-and-jump events, the jump length j is positively correlated with the slope s ($r = 0.63$), indicating that larger beads are looser (Figure 2D). This also proves that larger j values arise from the unfolding of larger structures rather than the simultaneous unfolding of the same structures. Consistently, the slope s is anticorrelated ($r = -0.25$) with the waiting time τ (Figure 2E) because looser beads (larger s) are expected to unfold faster (shorter τ). The jump length j is anticorrelated with the waiting time τ ($r = -0.21$) (Figure 2F), which indicates that the smaller the collapsed structure is, the denser and more stable the structure is. On the other hand, chain rigidity limits the generation of the infinitesimal size of collapsed structures. A decrease in bead density and stability with increasing bead size could result from the rearrangement and defects introduced during adjacent mergence. To further evaluate the reproducibility of our experimental results, PNIPAM globules were also unfolded under a stretching force of 3 pN (R0-T3). Consistently, j, τ, s, and their correlation followed the same trend (Table S1, Figures S2, and S3).

Force-Induced Unfolding of the Collapsed Globule Formed by the Salt-Driven Coil−Globule Transition (R0-S6). We further investigated the salt-driven transition of PNIPAM. Before stretching, the buffer was changed to 0.3 M Na$_2$SO$_4$ and stabilized for at least 20 min. Then, the collapsed globule was stretched at a constant force of 6 pN to unfold (R0-S6). Similarly, the salt-driven collapse also showed discontinuous wait-and-jump steps (Figure S4). The jump length shows quantized distribution with a minimum value of 7.6 ± 1.2 nm (the first peak in Figure 3A), which is equivalent to 30 ± 5 repeat units (Figure 3A and Table S2).

The prior waiting time τ was found to similarly follow a multiexponential distribution (at least two exponents) (Figure 3B). Moreover, the expansive slope was found to be exponentially distributed as well (Figure 3C). The slope s remained positively correlated with the jump length j ($r = 0.24$) (Figure 3D) and negatively correlated with the waiting time τ ($r = -0.26$) (Figure 3E), and the jump length j remained negatively correlated with the waiting time τ ($r = -0.31$) (Figure 3F). However, some differences were observed between the temperature- and salt-driven collapsed structures.
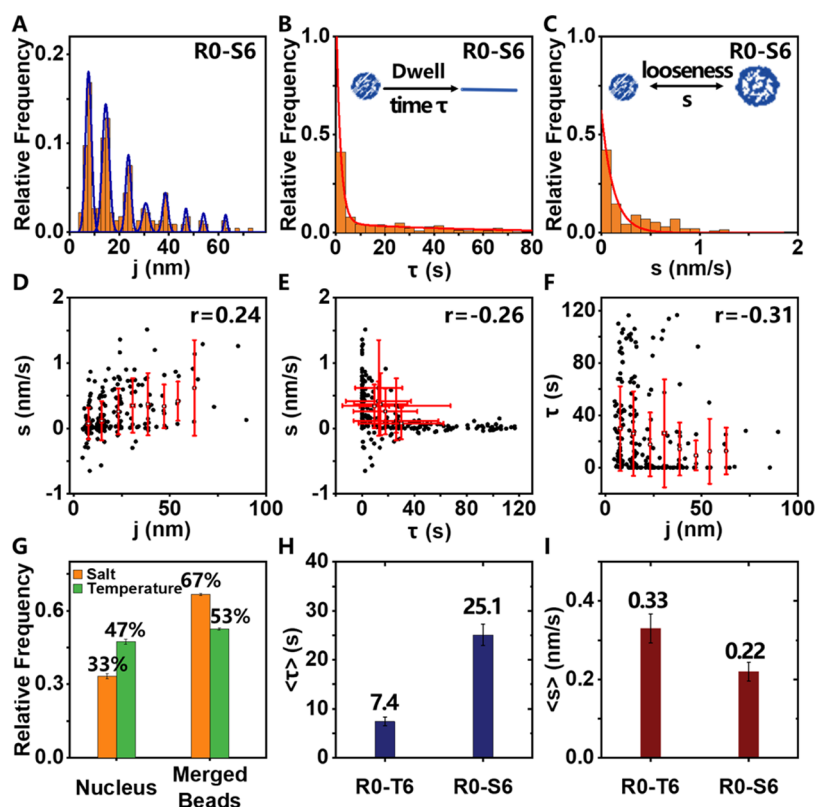
Figure 3. Statistical analysis of the unfolding parameters of salt-driven collapsed PNIPAM and a comparison with temperature-driven parameters. The unfolding experiment was performed under a constant force of 6 pN (R0-S6). (A−C) Histograms of the jump length j, waiting time τ, and expansive slope s from 226 jump events. The blue lines in (A) show Gaussian fits. The red lines in (B) and (C) show exponential fits. (D−F) Correlation plots and Pearson's correlation coefficients (r) of $j − s$, $\tau − s$, and $j − \tau$ from collapsed polymers. Each black dot indicates one wait-and-jump event. The open red squares indicate averages from each peak position in panel (A). The x and y error bars correspond to the standard deviations. (G) Relative frequency of salt-driven (R0-S6) and temperature-driven (R0-T6) collapsed nuclei and merged beads. (H, I) Histograms of the average waiting time $\langle\tau\rangle$ and average slope $\langle s\rangle$ from salt-driven (R0-S6) and temperature-driven (R0-T6) collapsed polymers. Error bars indicate the standard error of the mean.

The frequency of forming the basic nucleus was lower for the salt-driven collapse (33 ± 1%) than for the temperature-driven collapse (47 ± 1%). The frequency of merged beads by the salt-driven collapse (67 ± 1%) was higher than that formed by the temperature-driven collapse (53 ± 1%) (Figure 3G). These results showed that temperature is more conducive to the formation of nuclei, while salt is more conducive to the formation of merged beads. In addition, the average lifetime of the salt-driven collapsed structure (25.1 ± 2.2 s) was more than 3 times longer than that of the temperature-driven one (7.4 ± 0.9 s) (Figure 3H and Table 2).

These results indicate that the collapsed structure formed under high salt at room temperature is more stable than that formed in pure water above LCST under our experimental conditions. The average slope $\langle s\rangle$ of the salt-driven collapsed structures was 0.22 ± 0.02 nm s^{-1}, which is smaller than that of the temperature-driven structure (0.33 ± 0.04 nm s^{-1}) (Figure 3I). In addition, 15% negative slopes were observed for R0-S6, which is obviously higher than the 6% negative slopes observed for R0-T6. These results show that the high-salt solution can produce tighter PNIPAM beads.

Effects of the External Force on the Coil−Globule Transition (R2-S6). Because PNIPAM-based smart materials (e.g., artificial muscles) may be used under an external load, it is important to know what effect does the force have on the coil−globule transition. To determine this information, the coil−globule transition was induced under an external force of

Table 2. Influences of Different Collapsing Methods and the External Force on Correlation Coefficients (r), the Average Waiting Time $\langle\tau\rangle$, and Average Slope $\langle s\rangle$

collapse method	temperature-driven (T)		salt-driven (S)	
relax force (pN)	0	0	0	2
stretch force (pN)	6	3	6	6
$r(j − s)$	0.63	0.24	0.24	0.32
$r(\tau − s)$	−0.25	−0.26	−0.26	−0.51
$r(j − \tau)$	−0.21	−0.31	−0.31	−0.13
$\langle\tau\rangle$ (s)	7.4 ± 0.9	8.4 ± 0.9	25.1 ± 2.2	25.4 ± 2.2
$\langle s\rangle$ (nm s^{-1})	0.33 ± 0.04	0.18 ± 0.02	0.22 ± 0.02	0.21 ± 0.02

2 pN in 0.3 M Na$_2$SO$_4$, and then the collapsed polymer was unfolded at 6 pN (R2-S6) (Figure 4A). Similar to those formed via the coil−globule transition without an external force, the as-formed structures also exhibited discontinuous jump steps during the unfolding (Figure S5). According to Figure S5, the collapsed chain behavior in response to the tensile force of 6 pN consists of a first sharp length increment, which corresponds to the unraveling of the collapsed globule to the beads-on-a-string structure, followed by the stepwise unfolding of single/multiple nuclei. In the investigated
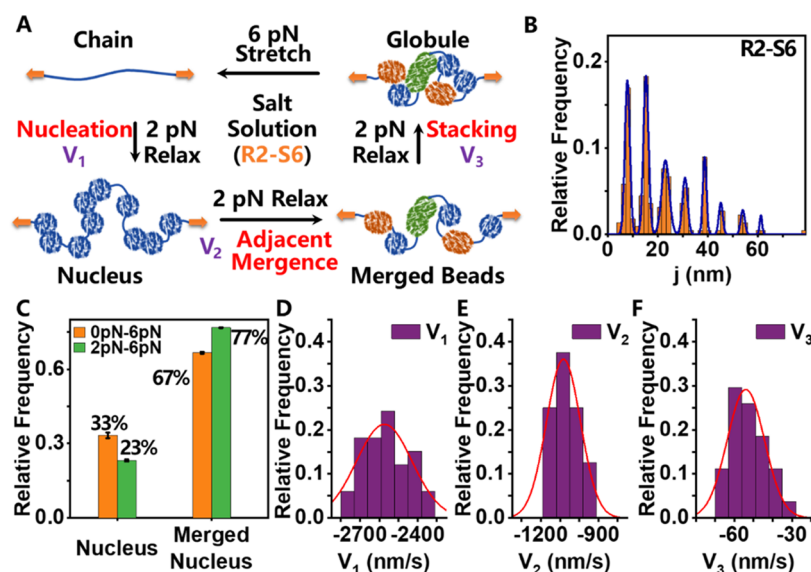
Figure 4. Effects of the external force on the coil−globule transition. (A) Diagram of the stretching response of a salt-driven collapsed polymer. The single PNIPAM collapsed at an external force of 2 pN and unfolded at a 6 pN constant force (R2-S6). (B) Histograms of the jump length j from 224 jump events. The blue lines show Gaussian fits. (C) Relative frequency of nuclei and merged beads formed by the salt-driven collapse under different external forces (0 and 2 pN). The orange columns correspond to polymers collapsed at 0 pN and unfolded at a constant force of 6 pN (R0-S6). The green columns correspond to polymers collapsed at 2 pN and unfolded at a constant force of 6 pN (R2-S6). Error bars indicate the standard error of the mean. (D−F) Histograms of the salt-driven collapse rate under 2 pN. The Gaussian fits (red lines) produce the most probable nucleation rate of $V_1 = (−2564.0 \pm 115.3, n = 33)$ nm s^{-1}, adjacent merging rate of $V_2 = (−1064.2 \pm 85.3, n = 8)$ nm s^{-1}, and stacking rate of $V_3 = (−52.5 \pm 8.8, n = 27)$ nm s^{-1}. The minus sign before the number represents the collapsing (shortening) of the polymer chain.
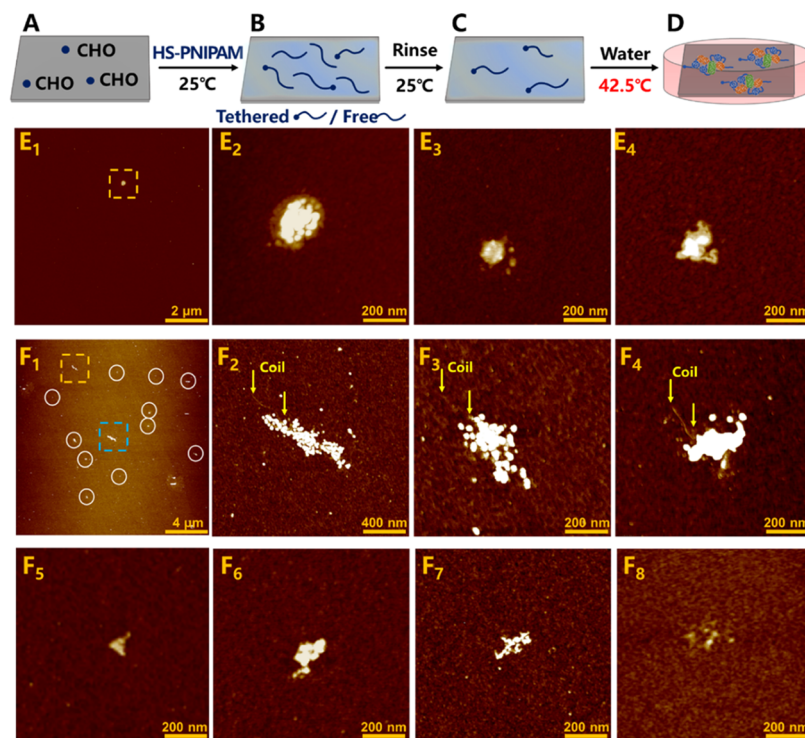
Figure 5. AFM imaging of individual PNIPAM chains above LCST. (A−C) Scheme of covalent immobilization of individual PNIPAM molecules on a solid substrate. The physically adsorbed PNIPAM was removed by vigorous rinsing with water at room temperature. (D) Immobilized sample was incubated in pure water at 42.5 °C to induce the coil−globule transition. (E$_1$−E$_4$) Representative AFM images of globules containing the nuclei and merged beads. The panel (E$_2$) shows a magnified image of the dashed box in (E$_1$). (F$_1$−F$_4$) AFM images of globules containing free chains (yellow arrows) and merged beads (nuclei). The panel (F$_2$) and (F$_3$) show magnified images of the yellow and blue dashed boxes in (F$_1$). The white circles in (F$_1$) represent shorter PNIPAM chains that contain a smaller number of collapsed nuclei and beads (F$_5$−F$_8$). The height scale bar for (E$_1$)−(E$_4$) is 10 nm and for (F$_1$)−(F$_8$) is 4 nm.

condition, the contribution of individual or merged nuclei to the whole structure of the globule can be estimated to be about 45%, indicating the presence of PNIPAM segments that have not collapsed within the globule.

The length of the nucleus, in this case, was 7.8 ± 1.0 nm, which is equivalent to 31 ± 4 repeat units. The lengths of larger collapsed structures were still multiples of the length of the nucleus (Figure 4B and Table S3). This finding indicates that the size of the nucleus and the adjacent mergence process were not affected by a 2 pN force during the collapse. Interestingly, the 2 pN external force somehow facilitated the formation of merged beads since the proportion of merged beads increased from $67 \pm 1\%$ (zero force) to $77 \pm 0.5\%$ (2 pN pulling force) (Figure 4C). This may be ascribed to the fact that small external forces can interfere with the stability of the nucleus (or bead) and improve the mobility of the chain to facilitate adjacent mergence. The prior waiting time τ still followed a multiexponential distribution (Figure S6), and the average waiting time $\langle \tau \rangle$ was found to be 25.4 s (R2-S6), which is very close to that without the external force (25.1 s) (R0-S6). This result demonstrates that the external force during collapse has no obvious effect on the stability of the collapsed structures. The expansive slope remained exponentially distributed (Figure S7), and the correlations of $j - s$, $\tau - s$, and $j - \tau$ showed the same trend as that without the external force (R0-S6) (Figure S8 and Table 2).

Collapse Rates of the Coil–Globule Transition. The extension–time collapsing curves show multiple descending steps (Figure S9) with different descent rates. We calculated the slope of extension–time trajectories that represent the collapse rate V (SI Section 1.14, Figures S9, and S10). The statistical results show that all of the collapse rates were clustered in three distinct regions, namely, fast collapse rates $V_1 = (-2564.0 \pm 115.3)$ nm s^{-1} (Figure 4D), medium collapse rates $V_2 = (-1064.2 \pm 85.3)$ nm s^{-1} (Figure 4E), and slow collapse rates $V_3 = (-52.5 \pm 8.8)$ nm s^{-1} (Figure 4F). According to the sequence of their occurrence, these three rates can be ascribed to nucleation (V_1), adjacent mergence (V_2), and bead stacking (V_3). The collapse curve of nucleation and adjacent mergence is basically a single-step process. However, the collapse curve of V_3 is discontinuous with fluctuations (Figure S9), which indicates that there is no strong interaction between the beads, and this may be the reason that beads finally do not rearrange into one uniform compact globule. For the stacking of distant beads, due to steric hindrance, it is difficult for the defect areas to interact and merge with each other.

Direct Observation of the Subtle Structure of a Collapsed PNIPAM Chain by AFM Imaging. SMFS experiments showed that above the LCST, the PNIPAM globule is not a uniform compact globule but contains a mixture of beads of variable sizes. To confirm this result, we used AFM imaging to visualize the actual structure of the globule. AFM imaging of a single-chain PNIPAM has traditionally been considered a challenge. The high capability of a flexible polymer to spread results in an extremely flat profile.[43] The individual polymers are indistinguishable from the substrate because their height is comparable to the substrate roughness and the finite dimensions of the tip.[43,44] To observe the structure of the collapsed globule, the PNIPAM molecules were covalently tethered on the substrate from its dilute solution $(10^{-8} \text{ g mL}^{-1})$ via silanization, aldimine condensation, and thioacetal reaction at a low density to prevent intermolecular aggregation (Figure 5A, SI Section 1.16, Figures S11, and S12). It should be emphasized that since water is a good solvent for PNIPAM at 25 °C, the nontethered free chain can be removed easily by rinsing, and the covalently immobilized chain exists in an isolated state here (Figures 5B,C and S12), and intermolecular aggregation does not occur owing to the very low surface density of PNIPAM (Figure $5E_1, F_1$).

To study the globule structures, the immobilized PNIPAM was incubated in warm water (42.5 °C) to induce the coil–globule transition. The sample was then dried before AFM imaging in air. Figure 5E shows representative AFM images, and free PNIPAM segments with merged beads can be observed in the collapsed globule (Figure $5E_1$–E_4, F_1–F_8). This finding is in good agreement with the earlier study by Wu et al.[45,46] The results also show similar stacking structures with orientation (Figure $5F_1$–F_4), which may be induced by the moving gas–liquid interface when the PNIPAM-immobilized substrate is removed from the water.[43] This result is consistent with the weak interactions among the merged beads as detected by SMFS experiments. As shown in Figure $5F_1$, due to the molecular weight distribution (Figure S15, SI), PNIPAM chains with different lengths will collapse to form globule structures containing different numbers of beads and nuclei. Figure $5F_2, F_3$ shows two PNIPAM chains with higher molecular weight, which form ~50 to 60 beads (nuclei) as judged from the number of white dots in the two AFM images. Because there are ~23% PNIPAM chains that exhibit a molecular weight of ≥ 200 kg mol^{-1} (which can form ≥ 47 nuclei), the number of beads (nuclei) observed in Figure $5F_2, F_3$ is reasonable, while many other shorter PNIPAM chains form collapsed globules with a smaller number of beads/nuclei, as shown in Figure $5F_5$–F_8.

■ CONCLUSIONS

Using magnetic tweezers and AFM imaging, peculiar features of the PNIPAM single chain in the globular state were detected for the first time. The transition can be divided into three steps: rapid nucleation, medium-speed adjacent mergence, and the slow bead stacking process. Interestingly, the size of the nucleus is not random but corresponds to ~31 repeat units. This finding is in good agreement with some recent theoretical simulations, which showed that the PNIPAM chain with less than ~31 repeating units is too short to form a stable fold.[38−41] The subsequent transition undergoes a previously undiscovered process of adjacent mergence in which adjacent structures combine to form merged beads, while the nonadjacent nuclei barely participate in the mergence process. The good agreement between the measured and expected lengths for merged beads (Tables S1−S3) indicates the small gap in between adjacent beads just before the mergence. Considering the random nucleation location along the PNIPAM chain, the original gap in between newly formed nuclei/beads may be big. However, according to previous simulations, such nuclei/beads are quite mobile, which can reduce the gap between the neighboring nuclei/beads, and permit shape fluctuations that allow the merging of adjacent nuclei/beads.[47] This hypothesis can be further supported by the fact that the probability of formation of bigger beads gets decreased greatly (Figures 2A, 3A, 4A), since the mobility of bigger beads along the string will get more difficult, making it difficult for the beads to meet and merge. The final collapsed globule is composed of stacked beads of different sizes but is not a uniform, compact globule.

These new findings are quite different from the traditional theory where unwound segments aggregated into only one uniform globule.[11−14] Under the effect of both salt and thermal stimuli, PNIPAM undergoes the same collapse process, which can be regarded as an inherent property (due to the presence of both hydrophobic and hydrogen-bonding interactions). We name this collapse process composed of nucleation, adjacent mergence, and stacking as the NAS transition.

Interestingly, the merged beads exhibit different mechanical stabilities. The larger the merged bead is, the looser and less stable the merged structure is. Temperature is more conducive to nucleation, while salt is more conducive to the formation of merged beads. Furthermore, the salt-driven collapsed structures formed at room temperature are more compact and stable than the temperature-driven collapsed structures formed above LCST under our experimental conditions, which may result in higher stress properties. In addition, applying a certain degree of pulling force during collapsing can somehow control the nuclei/merged bead structures. This indicates that the mechanical property of PNIPAM-based materials can be tuned by external stimuli.

Compared with AFM-based single-molecule force spectroscopy, magnetic tweezers exhibit many advantages. For example, the 3D free rotating magnetic bead allows the exclusion of multiple molecules stretching (Figure S20). The surface detachment of the polymer chain in the form of multiple polymer loops or train structures, which may also produce multiple length/force steps in the extension−time or force−distance curves, can be identified and excluded easily (Figure S21). Furthermore, the higher force sensitivity and long-term stability allow the investigation of weak molecular interactions and slow processes. Therefore, this work provides a new and universal research method for the study of a basic problem of polymer science, namely, the polymer coil−globule transition, especially for the globule structure with lower mechanical stability. The transition kinetics revealed in this work provides the most profound understanding of the PNIPAM coil−globule transition thus far, which will be beneficial to the fine-tuning of the stimuli-responsive properties of PINPAM-based materials. For example, to increase the response speed and mechanical stability of the materials, we can use shorter PNIPAM chains (e.g., containing ∼31 repeating units) in the matrix. We believe that in the near future, this research method will bring new breakthroughs to the study of other important polymer behaviors, such as the glass transition and the nucleation of polymer crystallization.

■ EXPERIMENTAL SECTION

Dual functionalized PNIPAM, with carboxyl and thiol groups at its two ends, was prepared by reversible addition fragmentation chain-transfer (RAFT) polymerization (more details on the Synthesis and Characterization of PNIPAM section can be found in the Supplementary Information, and Figures S13−S16). The phase transition temperature (LCST) of PNIPAM was determined to be 30.5 °C in 10 mM phosphate-buffered saline (PBS) solution (Figure S17). To perform the single-molecule magnetic tweezers (MT) experiment, the PNIPAM was bridged in between the magnetic particle and glass substrate via covalent coupling (see the SI for more details). MT (Biophysical Scientific Instrument Inc., Singapore) was used for single PNIPAM manipulation (Figure S18) using a homemade sample heating stage for temperature control (Figures S18 and S19). The single-molecule experiment involving the temperature-driven collapse (T) was performed in 10 mM PBS at 42.5 ± 0.5 °C, and that involving the salt-driven collapse (S) was performed in a 0.3 M Na_2SO_4 solution at room temperature. The manipulation of PNIPAM was initiated after a stabilization time of at least 20 min. During the constant-force experiment under two conditions (T, S), the polymer chain was allowed to collapse at no (or low) external force for 120 s, then the collapsed chain was unfolded at a high force for 600 s, and the procedure was repeated. Details of the materials and methods are provided in Supporting Text Section 1. To minimize the PNIPAM-interface interactions, 1% Tween-20 was introduced in the buffer solution, and the UV experiments showed that it did not affect the LCST of PNIPAM (Figure S18). Control experiments on multipolymer tethering and the desorption of a polymer chain from the substrate or the magnetic particle are shown in Figures S20 and S21. The stretching and unfolding of a free polymer with a collapsed intrachain structure is shown in Figure S22.

■ ASSOCIATED CONTENT

Ⓢ Supporting Information

The Supporting Information is available free of charge at https://pubs.acs.org/doi/10.1021/acs.macromol.2c01039.

Additional experimental details, materials, and methods, including photographs of the experimental setup; typical stretching−relaxation curves for all MT experiments; statistical analysis data of the unfolding parameters for all MT experiments; AFM imaging; ^1H NMR spectra; GPC; UV−vis spectra; transmittance; and homemade heating apparatus (PDF)

■ AUTHOR INFORMATION

Corresponding Author

Wenke Zhang − *State Key Laboratory of Supramolecular Structure and Materials, College of Chemistry, Jilin University, Changchun 130012, China;* ⓞ orcid.org/0000-0002-4569-6035; Email: zhangwk@jlu.edu.cn

Authors

Jianyu Liu − *State Key Laboratory of Supramolecular Structure and Materials, College of Chemistry, Jilin University, Changchun 130012, China;* ⓞ orcid.org/0000-0002-5289-2739

Huazhang Guo − *Institute of Nanochemistry and Nanobiology, Shanghai University, Shanghai 200444, China*

Qingjie Gao − *State Key Laboratory of Supramolecular Structure and Materials, College of Chemistry, Jilin University, Changchun 130012, China*

Hongbin Li − *Department of Chemistry, University of British Columbia, Vancouver V6T 1Z4, Canada;* ⓞ orcid.org/0000-0001-7813-1332

Zesheng An − *State Key Laboratory of Supramolecular Structure and Materials, College of Chemistry, Jilin University, Changchun 130012, China;* ⓞ orcid.org/0000-0002-2064-4132

Complete contact information is available at:
https://pubs.acs.org/10.1021/acs.macromol.2c01039

Author Contributions

The manuscript was written through contributions of all authors. All authors have given approval to the final version of the manuscript.

Notes

The authors declare no competing financial interest.

REFERENCES

(1) Nishio, I.; Sun, S.-T.; Swislow, G.; Tanaka, T. First observation of the coil-globule transition in a single polymer chain. *Nature* **1979**, *281*, 208−209.

(2) Fernandez, J. M.; Li, H. Force-clamp spectroscopy monitors the folding trajectory of a single protein. *Science* **2004**, *303*, 1674−1678.

(3) Everaers, R.; Sukumaran, S. K.; Grest, G. S.; Svaneborg, C.; Sivasubramanian, A.; Kremer, K. Rheology and microscopic topology of entangled polymeric liquids. *Science* **2004**, *303*, 823−826.

(4) Hu, D.; Yu, J.; Wong, K.; Bagchi, B.; Rossky, P. J.; Barbara, P. F. Collapse of stiff conjugated polymers with chemical defects into ordered, cylindrical conformations. *Nature* **2000**, *405*, 1030−1033.

(5) Juodkazis, S.; Mukai, N.; Wakaki, R.; Yamaguchi, A.; Matsuo, S.; Misawa, H. Reversible phase transitions in polymer gels induced by radiation forces. *Nature* **2000**, *408*, 178−181.

(6) Michalska-Walkowiak, J.; Förster, B.; Hauschild, S.; Förster, S. Bistability, remanence, read/write-memory, and logic gate function via a stimuli-responsive polymer. *Adv. Mater.* **2022**, *34*, No. 2108833.

(7) Sun, J.; Rijpkema, S. J.; Luan, J.; Zhang, S.; Wilson, D. A. Generating biomembrane-like local curvature in polymersomes via dynamic polymer insertion. *Nat. commun.* **2021**, *12*, No. 2235.

(8) Gunari, N.; Balazs, A. C.; Walker, G. C. Force-induced globule-coil transition in single polystyrene chains in water. *J. Am. Chem. Soc.* **2007**, *129*, 10046−10047.

(9) Li, I. T. S.; Walker, G. C. Interfacial free energy governs single polystyrene chain collapse in water and aqueous solutions. *J. Am. Chem. Soc.* **2010**, *132*, 6530−6540.

(10) Halperin, A.; Kröger, M.; Winnik, F. M. Poly(N-isopropylacrylamide) phase diagrams: fifty years of research. *Angew. Chem., Int. Ed.* **2015**, *54*, 15342−15367.

(11) Wu, C. *"Transition of Chain Conformation in Macromolecular Solutions" in Macromolecular Solutions*; Higher Education Press, 2021; Chapter 8, pp 335−391.

(12) Xu, J.; Zhu, Z.; Luo, S.; Wu, C.; Liu, S. First observation of two-stage collapsing kinetics of a single synthetic polymer chain. *Phys. Rev. Lett.* **2006**, *96*, No. 027802.

(13) Dahanayake, R.; Dormidontova, E. E. Hydrogen bonding sequence directed coil-globule transition in water soluble thermoresponsive polymers. *Phys. Rev. Lett.* **2021**, *127*, No. 167801.

(14) Quoika, P. K.; Fernandez-Quintero, M. L.; Podewitz, M.; Hofer, F.; Liedl, K. R. Implementation of the freely jointed chain model to assess kinetics and thermodynamics of thermosensitive coil-globule transition by markov states. *J. Phys. Chem. B* **2021**, *125*, 4898−4909.

(15) Li, I. T. S.; Walker, G. C. Signature of hydrophobic hydration in a single polymer. *Proc. Natl. Acad. Sci. U.S.A.* **2011**, *108*, 16527−16532.

(16) Liu, J.; Feng, W.; Zhang, W. A single-molecule study reveals novel rod-like structures formed by a thrombin aptamer repeat sequence. *Nanoscale* **2020**, *12*, 4159−4166.

(17) Grandbois, M.; Beyer, M.; Rief, M.; Clausen-Schaumann, H.; Gaub, H. E. How strong is a covalent bond? *Science* **1999**, *283*, 1727−1730.

(18) Zhang, X.; Kou, X.; Zhang, W.; Zhang, W. Identification of the new type of G-quadruplex with multiple vacant sites in human telomeric DNA. *CCS Chem.* **2021**, *3*, 3023−3035.

(19) Tian, Y.; Cao, X.; Li, X.; Zhang, H.; Sun, C.; Xu, Y.; Weng, W.; Zhang, W.; Boulatov, R. A polymer with mechanochemically active hidden length. *J. Am. Chem. Soc.* **2020**, *142*, 18687−18697.

(20) Xue, Y.; Li, X.; Li, H.; Zhang, W. Quantifying thiol−gold interactions towards the efficient strength control. *Nat. Commun.* **2014**, *5*, No. 4348.

(21) Bustamante, C. J.; Chemla, Y. R.; Liu, S.; Wang, M. D. Optical tweezers in single-molecule Biophysics. *Nat. Rev. Methods Primers* **2021**, *1*, No. 25.

(22) Kutnyanszky, E.; Embrechts, A.; Hempenius, M. A.; Vancso, G. J. Is there a molecular signature of the LCST of single PNIPAM chains as measured by AFM force spectroscopy? *Chem. Phys. Lett.* **2012**, *535*, 126−130.

(23) Cui, S.; Pang, X.; Zhang, S.; Yu, Y.; Ma, H.; Zhang, X. Unexpected temperature-dependent single chain mechanics of poly(N-isopropyl-acrylamide) in water. *Langmuir* **2012**, *28*, 5151−5157.

(24) Liang, X.; Nakajima, K. Nanofishing of a single polymer chain: temperature-induced coil-globule transition of poly (N-isopropylacrylamide) chain in water. *Macromol. Chem. Phys.* **2018**, *219*, No. 1700394.

(25) Kolberg, A.; Wenzel, C.; Hackenstrass, K.; Schwarzl, R.; Ruttiger, C.; Hugel, T.; Gallei, M.; Netz, R. R.; Balzer, B. N. Opposing temperature dependence of the stretching response of single PEG and PNiPAM polymers. *J. Am. Chem. Soc.* **2019**, *141*, 11603−11613.

(26) Haupt, B. J.; Senden, T. J.; Sevick, E. M. AFM evidence of rayleigh instability in single polymer chains. *Langmuir* **2002**, *18*, 2174−2182.

(27) Koster, D. A.; Palle, K.; Bot, E. S. M.; Bjornsti, M. A.; Dekker, N. H. Antitumour drugs impede DNA uncoiling by topoisomerase I. *Nature* **2007**, *448*, 213−217.

(28) Lipfert, J.; Kerssemakers, J. W. J.; Jager, T.; Dekker, N. H. Magnetic torque tweezers: Measuring torsional stiffness in DNA and RecA-DNA filaments. *Nat. Methods* **2010**, *7*, 977−980.

(29) Liu, C.; Kubo, K.; Wang, E.; Han, K. S.; Yang, F.; Chen, G.; Escobedo, F. A.; Coates, G. W.; Chen, P. Single polymer growth dynamics. *Science* **2017**, *358*, 352−355.

(30) Manosas, M.; Perumal, S. K.; Croquette, V.; Benkovic, S. J. Direct observation of stalled fork restart via fork regression in the T4 replication system. *Science* **2012**, *338*, 1217−1220.

(31) del Rio, A.; Perez-Jimenez, R.; Liu, R.; Roca-Cusachs, P.; Fernandez, J. M.; Sheetz, M. P. Stretching single talin rod molecules activates vinculin binding. *Science* **2009**, *323*, 638−641.

(32) Bauer, M. S.; Gruber, S.; Hausch, A.; Gomes, P.; Milles, L. F.; Nicolaus, T.; Schendel, L. C.; Navajas, P. L.; Procko, E.; Lietha, D.; Melo, M.; Bernardi, R. C.; Gaub, H. E.; Lipfert, J. A tethered ligand assay to probe SARS-CoV-2: ACE2 interactions. *Proc. Natl. Acad. Sci. U.S.A.* **2022**, *119*, No. e2114397119.

(33) Wang, Y.; Yao, M.; Baker, K. B.; Gough, R. E.; Le, S.; Goult, B. T.; Yan, J. Force-dependent interactions between talin and full-length vinculin. *J. Am. Chem. Soc.* **2021**, *143*, 14726−14737.

(34) You, H.; Wu, J.; Shao, F.; Yan, J. Stability and kinetics of C-MYC promoter G-quadruplexes studied by single-molecule manipulation. *J. Am. Chem. Soc.* **2015**, *137*, 2424−2427.

(35) Jacobson, D. R.; McIntosh, D. B.; Stevens, M. J.; Rubinstein, M.; Saleh, O. A. Single-stranded nucleic acid elasticity arises from internal electrostatic tension. *Proc. Natl. Acad. Sci. U.S.A.* **2017**, *114*, 5095−5100.

(36) Lv, S.; Dudek, D. M.; Cao, Y.; Balamurali, M. M.; Gosline, J.; Li, H. Designed biomaterials to mimic the mechanical properties of muscles. *Nature* **2010**, *465*, 69−73.

(37) Cao, Y.; Li, H. Engineered elastomeric proteins with dual elasticity can be controlled by a molecular regulator. *Nat. Nanotechnol.* **2008**, *3*, 512−516.

(38) Bejagam, K. K.; An, Y.; Singh, S. K.; Deshmukh, S. A. Machine-learning enabled new insights into the coil-to-globule transition of thermosensitive polymers using a coarse-grained model. *J. Phys. Chem. Lett.* **2018**, *9*, 6480−6488.

(39) Tavagnacco, L.; Zaccarelli, E.; Chiessi, E. On the molecular origin of the cooperative coil-to-globule transition of poly(N-isopropylacrylamide) in water. *Phys. Chem. Chem. Phys.* **2018**, *20*, 9997−10010.

(40) Abbott, L. J.; Stevens, M. J. A temperature-dependent coarse-grained model for the thermoresponsive polymer poly(N-isopropylacrylamide). *J. Chem. Phys.* **2015**, *143*, No. 244901.

(41) de Oliveira, T. E.; Netz, P. A.; Mukherji, D.; Kremer, K. Why does high pressure destroy co-non-solvency of PNIPAm in aqueous methanol? *Soft Matter* **2015**, *11*, 8599−8604.

(42) Petrov, A.; Kos, P.; Chertovich, A. Kinetic mechanisms of crumpled globule formation. *Soft Matter* **2020**, *16*, 2045−2054.

(43) Scotti, A.; Bochenek, S.; Brugnoni, M.; Fernandez-Rodriguez, M. A.; Schulte, M. F.; Houston, J. E.; Gelissen, A. P. H.; Potemkin, I. I.; Isa, L.; Richtering, W. Exploring the colloid-to-polymer transition for ultra-low crosslinked microgels from three to two dimensions. *Nat. Commun.* **2019**, *10*, No. 1418.

(44) Liu, J.; Wang, X.; Zhang, W. Atomic force microscopy imaging study of aligning DNA by dumbbell-like Au-Fe$_3$O$_4$ magnetic nanoparticles. *Langmuir* **2018**, *34*, 14875−14881.

(45) Wang, X.; Qiu, X.; Wu, C. Comparison of the coil-to-globule and the globule-to-coil transitions of a single Poly(N-isopropylacrylamide) homopolymer chain in water. *Macromolecules* **1998**, *31*, 2972−2976.

(46) Zhang, G.; Wu, C. Reentrant coil-to-globule-to-coil transition of a single linear homopolymer chain in a water / methanol mixture. *Phys. Rev. Lett.* **2001**, *86*, No. 822.

(47) Paul, S.; Majumder, S.; Das, S. K.; Janke, W. Effects of alignment activity on the collapse kinetics of a flexible polymer. *Soft Matter* **2022**, *18*, 1978−1990.